J Electr Eng Technol.2015;10(1):92-101
http://dx.doi.org/10.5370/JEET.2015.10.1.092

ISSN(Print) 1975-0102
ISSN(Online) 2093-7423

Power Quality Warning of High-Speed Rail Based on Multi-Features Similarity

Jingjing Bai*, Wei Gu†, Xiaodong Yuan, Qun Li**, Bing Chen** and Xuchong Wang***

Abstract – As one type of power quality (PQ) disturbance sources, high-speed rail (HSR) can have major impacts on the power supply grid. Providing timely and accurate warning information for PQ problems of HSR is important for the safe and stable operation of traction power supply systems and the power supply grid. This study proposes a novel warning approach to identify PQ problems and provide warning prompts based on the monitored data of HSR. To embody the displacement and status change of monitored data, multi-features of different sliding windows are computed. To reflect the relative importance degree of these features in the overall evaluation, an analytic hierarchy process (AHP) is used to analyse the weights of multi-features. Finally, a multi-features similarity algorithm is applied to analyse the difference between monitored data and the reference data of HSR, and PQ warning results based on dynamic thresholds can be analysed to quantify its severity. Cases studies demonstrate that the proposed approach is effective and feasible, and it has now been applied to an actual PQ monitoring platform.

Keywords: Multi-features similarity, Warning, Anomaly detection, AHP, Dynamic thresholds, Power quality (PQ), High-speed rail (HSR).

1. Introduction

As a new transportation means, high-speed rail (HSR) has introduced great economic and social benefits. However, the access of HSR exacerbates the power quality (PQ) and reduces the safety and reliability of the power supply grid. The primary PQ problems of electrified railways are widely believed to be harmonics, a low power factor and a large negative sequence current [1-3], but the loads of HSR increase considerably each year and cause stronger fluctuations and impacts. These results will complicate PQ problems of HSR, which increases the extent of PQ impact [4].

Conversely, the expansion in the scale and capacity of power systems has resulted in an increasing number of sensitive power consumers accessing these systems. These consumers request a higher PQ to ensure their normal operation [5, 6]. Therefore, monitoring and analysing the PQ status where large-scale HSRs access and taking effective measures to solve the deteriorated PQ problem are worthwhile endeavours. These methods are important to ensure safe operation of a power network.

At present, many studies have focused on analysing PQ characteristics of HSR [7-9]. Furthermore, most PQ researches also focused on the detection and identification of PQ disturbances and PQ evaluation [10-13]. Gupta et al. [10] proposed a recognition method for PQ disturbances that is based on continuous wavelet transform and feed-forward neural network. He et al. [11] proposed a real-time power quality disturbances classification by using S-transform and dynamics. Based on this hybrid method and a decision tree, PQ disturbances can be classified in a DSP-FPGA based hardware platform. Li et al. [12] proposed a synthetic evaluation method based on relative intensity entropy and local variable weight. This method could reflect the gradual change in the objective evaluation index weights with indicator values. Hai et al. [13] proposed an evaluation approach based on wavelet packet decomposition and fuzzy logic that mainly utilises a fuzzy model to amalgamate the redefined PQ indictors into one single index to facilitate synthetic evaluation.

Even though research on methods to mine PQ abnormal monitored data and provide warning prompts is lacking, the above survey indicates the development of a PQ monitored data acquisition system [14, 15] and previous studies provided the motivation to carry out the research study reported in this paper. In this study, we established a PQ warning approach based on multi-features similarity to analyse the abnormal severity of HSR PQ monitored data, and provide timely warning prompts for both the power suppliers and the railway authorities.

This paper is organised as follows. The PQ characteristics of HSR are presented in Section 2. The warning approach model and approach flow are presented in Section 3. The

† Corresponding Author: School of Electrical Engineering, Southeast University, China. (wgu@ seu.edu.cn)
* School of Electrical Engineering, Southeast University, China. ({jingjing_bai, xuchongw}@163.com)
** Jiangsu Electrical Power Company Research Institute, China. (lannyyuan@hotmail.com, qun_li@sina.com, cbsure@163.com)
Received: March 7, 2014; Accepted: October 2, 2014

numerical results and discussions are given in Section 4. In Section 5, the conclusions are presented.

2. The PQ Characteristics of HSR

A traction power supply system of HSR generally consists of an external power supply, traction substation, traction network, rail, etc. [16-18].

As a source of HSR energy, the external power supply mainly originates from the public power network. It is responsible for providing the high voltage for HSR, and its voltage grade often reaches 110 kV or 220 kV. The role of a traction substation is the conversion of electrical energy. Its core component is a traction transformer, such as a three-phase V/v connected to a traction transformer, impedance-matched balance traction transformer, etc. Traction networks directly supply power for HSR. Its rated voltage is often 27.5 kV or 55 kV. HSR is a special high-power and single-phase load, and the main PQ characteristics of HSR are as follows.

2.1 Harmonics

Harmonics of a HSR mainly originate from the AC-DC-AC converter or inverter in the power electronic equipment during operation [19]. The HSR generally features four major harmonic characteristics: 1) Three-phase harmonics are independent of each other; 2) Random, large and frequent fluctuations; 3) Harmonic vectors are widely distributed; 4) Under steady operation, the state of odd harmonics is worse than that of even harmonics.

2.2 Negative sequence current

Generally speaking, HSR traction loads are powered by two phases in a three-phase power system; thus, a negative sequence current that causes three-phase current unbalance can easily be generated. The value of the negative sequence current is related to the types of traction substations, distributions of trains and the values of traction loads.

Compared with ordinary electrified railways, the negative sequence currents of HSR have the following characteristics: 1) they increase significantly; 2) they last longer for high load rates and long HSR energising times.

2.3 Other PQ problems

The normal operation of HSR is vulnerable to random factors, such as switching the operating conditions, bends and climatic conditions. Almost all of these conditions bestow the characteristics of large and frequent fluctuations on traction loads and cause voltage variation at points of common coupling (PCC). The changes in the characteristics of traction loads of HSR are relatively smooth. Therefore, the resultant voltage fluctuation and flicker HSR are not serious [20]. Only some exceptional circumstances would cause these PQ problems to become so serious that they are worthy of attention.

3. Warning Approach for PQ Abnormal Monitored Data of HSR

Data mining of monitored data is necessary to analyse the PQ and control the HSR, particularly those circumstances that cause PQ anomalies during actual operation. Based on the existing PQ monitoring platform, this paper presents a PQ warning approach for HSR. First, to describe the displacement and status change of monitored waveform data, eight statistic features are computed via specific formulae for each feature. An analytic hierarchy process (AHP) is then used to analyse the weights of multi-features to reflect their relative importance degree in the subsequent similarity analysis. The Euclidean distance is obtained based on eight statistic features and their weights via a comparative analysis of the monitored waveforms and reference waveforms. Their similarity can be analysed according to the function of Euclidean distance. Finally, a warning grade to reflect the PQ anomalies severity of HSR can be obtained by setting the dynamic thresholds and the responding warning mechanism.

3.1 The computation of multi-features

In fact, the monitored waveform data in this study are a series of time sequences. In statistics, many features can be used to describe the displacement and status change of time sequences. After a general comparison among the characteristics of these features, eight statistic features are selected in this study. They are the minimum, maximum, average, variance, skewness, kurtosis, the product of skewness and kurtosis and the coefficient of variation. The computing methods of these features are introduced below.

The minimum, maximum and average are fundamental statistics features that can be used to describe the holistic displacement change of time sequences. Their analysis methods are routine computing formulas.

The variance is usually applied to describe the eccentricity between random variables and an average. It is widely computed using the following formula:

$$\sigma^2 = \frac{1}{N}\sum_{i=1}^{N}(x_i - u)^2 \ . \tag{1}$$

where μ is the average of the variable X; x_i is the i-th variable of the sliding window; N is the number of data points in the sliding window.

Skewness is a statistic that can describe the distribution symmetry of variate values [21, 22]. Its value can reflect the degree of deviation. The computation formula of

skewness is:

$$s_k = \begin{cases} g_1 = \dfrac{N \cdot \sum_{n=1}^{N} (x(n) - \hat{m})^3}{(N-1) \cdot (N-2) \cdot (\hat{\sigma})^3}, \\ \{E(g_1) - \dfrac{\sqrt{\mathrm{var}(g_1)}}{\sqrt{a}} \le g_1 \le E(g_1) + \dfrac{\sqrt{\mathrm{var}(g_1)}}{\sqrt{a}}\} \\ E(g_1) = 0, \\ \{-\infty \le g_1 \le E(g_1) - \dfrac{\sqrt{\mathrm{var}(g_1)}}{\sqrt{a}}, E(g_1) + \dfrac{\sqrt{\mathrm{var}(g_1)}}{\sqrt{a}} \le g_1 \le +\infty\} \end{cases} \quad (2)$$

where $x=\{x(n): n=1,2,\cdots\cdots, N\}$; g_1 is its unbiased estimate; $\hat{m}$ and $\hat{\sigma}$ are the average and the standard deviation of $x(n)$, respectively; a=1-q (q generally takes the value 0.95) ; The variance of g_1 is:

$$\mathrm{var}(g_1) = \frac{6 \cdot N \cdot (N-1)}{(N-2) \cdot (N+1) \cdot (N+3)}. \quad (3)$$

Kurtosis is a statistic that describes the degree of steepness of all variate distribution values. The skewness is computed as follows:

$$k_u = \begin{cases} g_2 = \dfrac{N \cdot (N+1) \cdot \sum_{n=1}^{N} (x(n) - \hat{m})^4}{(N-1) \cdot (N-2) \cdot (N-3) (\hat{\sigma})^4} - \dfrac{3 \cdot (N-1)^2}{(N-2) \cdot (N-3)}, \\ \{E(g_2) - \dfrac{\sqrt{\mathrm{var}(g_2)}}{\sqrt{a}} \le g_2 \le E(g_2) + \dfrac{\sqrt{\mathrm{var}(g_2)}}{\sqrt{a}}\} \\ E(g_2) = \dfrac{-6}{N-1}, \\ \{-\infty \le g_2 \le E(g_2) - \dfrac{\sqrt{\mathrm{var}(g_2)}}{\sqrt{a}}, E(g_2) + \dfrac{\sqrt{\mathrm{var}(g_2)}}{\sqrt{a}} \le g_2 \le +\infty\} \end{cases}, \quad (4)$$

where the variance of g_2 is:

$$\mathrm{var}(g_2) = \frac{24 \cdot N \cdot (N-1)^2}{(N-3) \cdot (N-2) \cdot (N+3) \cdot (N+5)}. \quad (5)$$

The coefficient of variation is the absolute value that can reflect a discrete level of data [23]. Its value is not only influenced by the discrete level of the variable value but also by the average of the variable value. The coefficient of variation is computed as follows:

$$CV = \frac{\sigma}{\mu}. \quad (6)$$

where μ is the average of the variable X; σ is the standard variance of the variable X.

In practical applications, the coefficient of variation can be used to eliminate influences generated by the difference in the units and the average when several variable values need to be compared. Therefore, the coefficient of variation can somewhat describe the status change of time sequences.

3.2 Analytic hierarchy process algorithm

The analytic hierarchy process (AHP) is an algorithm that is usually used to describe the degree of relative importance [24, 25]. In this study, the main parts to analyse weights based on the AHP are as follows:

3.2.1 Establish a judgment matrix.

The first step of the common AHP is the establishment of a multilayer hierarchical structure. However, the weights of different features need to be determined in this study, and they are at the same level. Hierarchical single arrangement is sufficient, and other complex multilayer hierarchical structures do not need to be established. Therefore, we can immediately proceed to the next step, the establishment of a judgment matrix.

In common AHP, the value of elements in the judgment matrix often uses a 1~9 scale method. However, many inappropriate applications exist in practice, which may result in wrong assessment results or incorrect consistency tests. Therefore, this study adopts the index scale shown in [24].

3.2.2 Check consistency.

If the judgment matrix is a second order matrix, the consistency does not need to be checked, and the weights comprise a normalised greatest eigenvector judgment matrix. However, the judgment matrix is not a second order matrix under normal circumstances, and the consistency needs to be checked.

The consistency ratio (CR) is used to assess the consistency. It can be obtained by dividing the coincidence indicator (CI) by the random consistency (RI). When the value of CR is less than 0.1, the results of a hierarchical single arrangement are consistent. Otherwise, the elements of the judgment matrix need to be recalculated.

3.3 Warning mechanism model

In statistics, Euclidean distance is often used to describe the difference between two time sequences [26, 27]. In this study, the weights are considered in the computation of the Euclidean distance as follows:

$$D_e = \sqrt{\sum_{j=1}^{n} [w_j (T_j - R_j)]^2}. \quad (7)$$

where n is the order of the matrix; w_j is the weight of the j-th feature; T_j is the j-th feature value of the different sliding window; R_j is the j-th feature value of the reference waveform data.

However, the Euclidean distance cannot clearly reflect the similarity between the monitored waveforms and reference waveforms. The function of the Euclidean distance is used to compute the similarity as follows:

$$S_i = \frac{D_e}{8 + D_e} . \tag{8}$$

After the similarity is calculated, thresholds that can be compared with the similarity need to be determined to reflect whether the similarity degree between the monitored waveforms and reference waveforms meets the warning requirement. However, setting static thresholds is insufficient because static thresholds cannot adjust for the normal jitter of monitored data at some time points, and their method of setting is inflexible. Therefore, dynamic thresholds are applied in PQ warning in this study as follows:

$$T_d = \alpha * T_s + (1 - \alpha) * t . \tag{9}$$

where T_d and T_s represent the dynamic thresholds and static thresholds, respectively; α is weight coefficient of the static threshold; t represents the fluctuation degree of the similarity waveform, which will take effect if the fluctuation degree achieves a certain level. Its specific computation formula is:

$$t = \begin{cases} k * k_u * s_k & , k_u * s_k \geq T \\ 0 & , k_u * s_k \leq T \end{cases} . \tag{10}$$

where k is the proportionality coefficient of the product; s_k is the skewness of different sliding windows; k_u is the kurtosis of different sliding windows; T is the threshold of the fluctuation degree, and its comparison object is the product of skewness and kurtosis.

In this study, two thresholds are computed according to the above method to execute a PQ warning. The number of data that exceeds the dynamic thresholds can be acquired by comparing the monitored data with the dynamic thresholds. The specific warning mechanism is:

Table 1. PQ Warning Mechanism

Grade of warning	Condition
Grade 2	$n_k \leq n_1$ and $n_k \leq n_2$
Grade 1	$n_k \geq n_1$ and $n_k \leq n_2$, $n_k \geq n_1$ and $n_k \leq n_2$
Normality	$n_k \geq n_1$ and $n_k \geq n_2$

where n_k is the number of limit-exceeding instances; n_1 and n_2 are the thresholds of the number of limit-exceeding instances, respectively, $n_1 \geq n_2$.

3.4 Implementation of the proposed approach

Before determining a warning, enough monitored data should be provided. If the number of data cannot meet the requirement of integrity, a warning detection will not be effective. In this study, 50% is used to serve as a data integrity limit. If the quantity of data falls below the threshold, the monitored data are invalid as a PQ warning. The main flowchart of the proposed approach is shown in Fig. 1.

The implementing process of the proposed approach is given as follows:

1) Use the PQ monitoring equipment to acquire the monitored waveform data from the traction substation side during HSR operation. Extract the required monitored data of the real-time monitored waveforms from the PQ monitoring platform in this study.
2) Judge the integrity of the monitored data.
   In this step, the number of PQ monitored data needs to be judged against the requirement of data integrity. If the requirement is met, proceed to Step 3. If not, the monitored data should be reselected.
3) According to the experience of the actual test, determine the length of the sliding window.
4) Based on the Formula (1)~(6), calculate the multi-features of different sliding windows.
5) Utilise the different features of all sliding windows and reference data to establish a multi-dimensional characteristic matrix. Then, the following Formula (11) can be used to standardise the multi-dimensional characteristic matrix and obtain its un-dimensioned characteristic matrix.

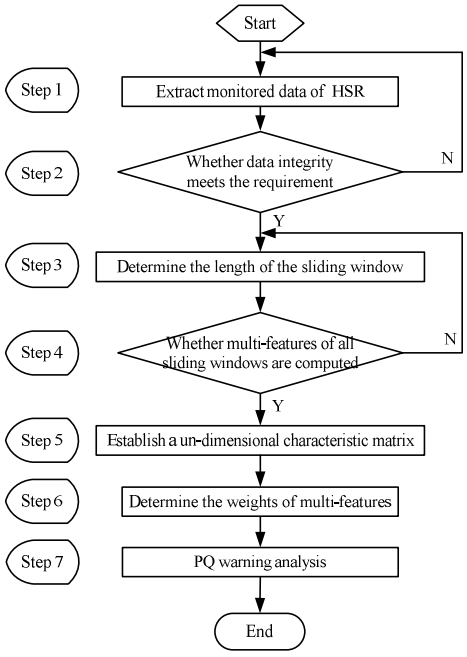

Fig. 1. Main flowchart of PQ warning

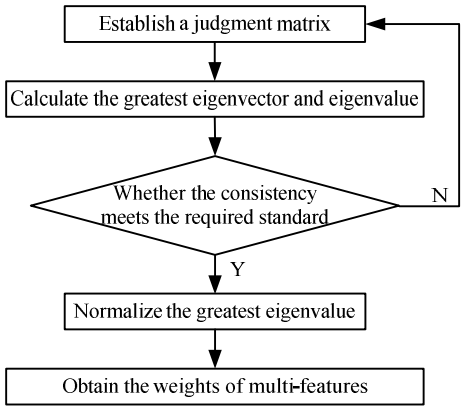

Fig. 2. Flowchart of determining the weights of multi-features

$$x_{ij}^{*}=\frac{x_{ij}-\overline{x_j}}{s_j}. \quad (11)$$

$$(i=1,2,\ldots,n; j=1,2,\ldots, n)$$

where $\overline{x_j}=\frac{1}{n}\sum_{i=1}^{n}x_{ij}$; $s_j=\sqrt{\frac{1}{n-1}\sum_{i=1}^{n}(x_{ij}-\overline{x_j})^2}$.

6) Use the AHP algorithm to determine the weights of multi-features. Its detailed flowchart is shown in Fig. 2.

From Fig. 2, the specific steps to analyse weights are as follows:

(1) Establish a judgment matrix based on the degree of relative importance of different features.
(2) Calculate the greatest eigenvector and the greatest eigenvalue of the judgment matrix.
(3) Check the consistency of the results of a hierarchical single arrangement. If the value of CR meets the required standard, proceed to Step (4). If not, the elements of the judgment matrix should be reselected.
(4) Normalize the greatest eigenvector.
(5) The weights can be obtained from the results of the normalisation.

7) According to the above computation results, a PQ warning analysis can be performed. Its detailed flowchart is shown in Fig. 3. The specific steps are as follows:

(1) Based on the weights and values of different features, the Euclidean distance between the monitored waveforms and reference waveforms can be computed.
(2) The function of Euclidean distance is then used to compute the similarity degree between them.
(3) The fluctuation degree of similarity waveform can be computed.
(4) The dynamic thresholds are computed according to the fluctuation status of the monitored waveform data.

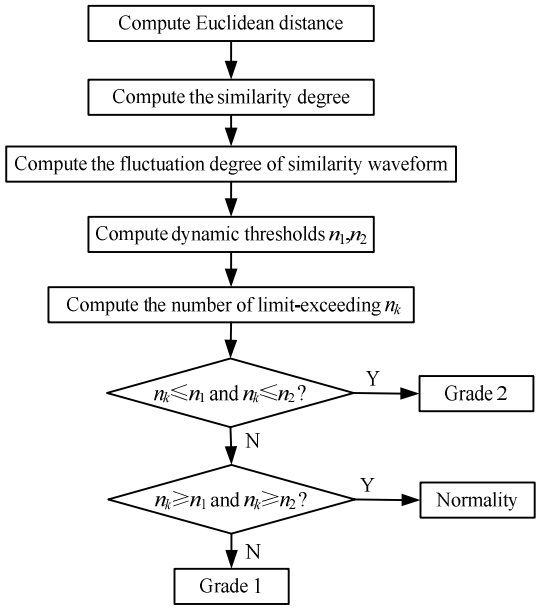

Fig. 3. Flowchart of PQ warning analysis

(5) Compute the number of limit-exceeding instances.
(6) Based on PQ warning mechanism, the severity of the anomalies of monitored data can be analysed and assigned a warning grade.

4. Case Studies

After several years of construction, Jiangsu province in China has established a standardised net-based PQ monitoring system. The system can provide the basic conditions for data collection, remote transmission, analysis and sharing. At present, the province has installed more than 1300 monitoring points and can monitor the PQ status of large impact loads, new energy sources and key substations.

Utilising the HSR PQ special monitoring platform that is part of the visual monitoring system, this study takes monitored waveform data from the 220 kV I-bus bar at the Shanqian traction substation of the Beijing-to-Shanghai high-speed rail from October 7th, 2013 as an example. The transformer of this traction substation uses three-phase V/v wiring, and the minimum short-circuit capacity of bus is 10638 MVA.

4.1 The multi-features of different sliding window

Many types of index data are collected in one monitored day. Some of these data were abnormal and needed to be given warning prompts, such as 31st harmonic current. Fig. 4 shows the original three-phase data waveforms of the 31st harmonic current. The following analysis of the warning algorithm and flow is based on this example in Fig. 4.

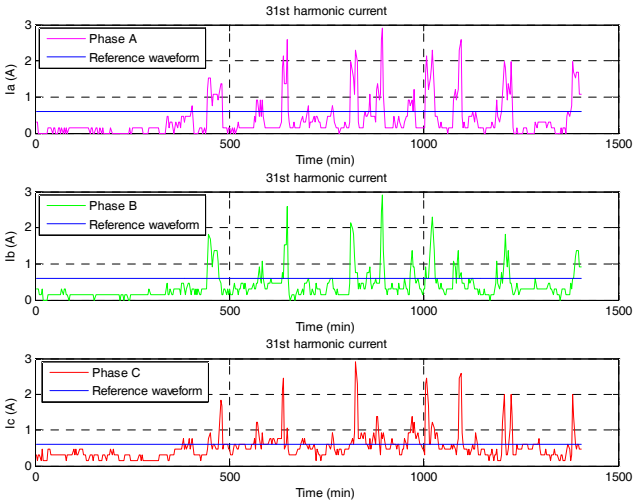

Fig. 4. The original data waveforms of 31st harmonic current

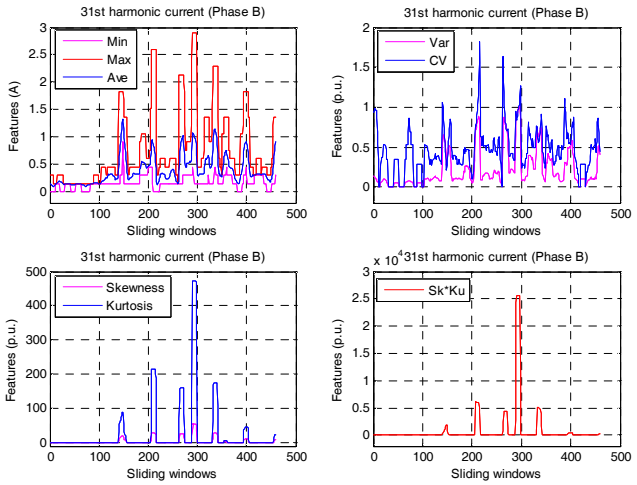

Fig. 5. Multi-features of different sliding windows before normalisation

According to the operating status of the monitored equipment, the 31st harmonic current can produce data every 3 minutes; thus, one day should generate 480 sets of data. In this case, the number of monitored data points is 468, which meets the requirement for data integrity and allows us to proceed to the next step.

Sliding windows are used to divide the entire waveform to help capture and analyse sudden changes in the value of monitored waveform data. In this case, after several cycles of debugging and analysis, we find that the results of debugging were improved by setting the length of the sliding window to 10. The multi-features of different sliding windows of Phase B for these circumstances are shown in Fig. 5.

In Fig. 5, the minimum, maximum and average are used to reflect the displacement change of monitored waveform data; the variance, skewness, kurtosis, the product of skewness and the coefficient of variation are used to reflect the status change of monitored waveform data.

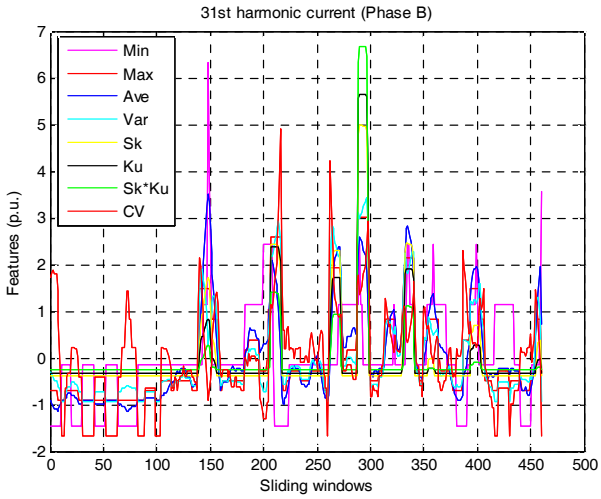

Fig. 6. Multi-features of different sliding windows after normalization

Formula (11) is used to eliminate the effect of multi-dimension. The results are shown in Fig. 6.

4.2 The weights of multi-features

When multi-features are given weights, the weights of the displacement change should be larger than the weights of the status change. This condition is necessary because the effect of the displacement change is more pronounced than the effect of the status change when the monitored waveforms are compared with reference waveforms. Therefore, the specific judgment matrix can be obtained as follows:

$$B=\begin{bmatrix} 1 & 1 & 1 & 1.3161 & 3 & 3 & 3 & 1.3161 \\ 1 & 1 & 1 & 1.3161 & 3 & 3 & 3 & 1.3161 \\ 1 & 1 & 1 & 1.3161 & 3 & 3 & 3 & 1.3161 \\ 0.7598 & 0.7598 & 0.7598 & 1 & 1.7321 & 1.7321 & 1.7321 & 1 \\ 0.3333 & 0.3333 & 0.3333 & 0.5773 & 1 & 1 & 1 & 0.5733 \\ 0.3333 & 0.3333 & 0.3333 & 0.5773 & 1 & 1 & 1 & 0.5733 \\ 0.3333 & 0.3333 & 0.3333 & 0.5773 & 1 & 1 & 1 & 0.5733 \\ 0.7598 & 0.7598 & 0.7598 & 1 & 1.7321 & 1.7321 & 1.7321 & 1 \end{bmatrix} \quad (12)$$

The judgment matrix shows the degree of the relative importance of different elements, and the row vectors of the matrix represent the minimum, maximum, average, variance, skewness, kurtosis, the product of skewness and kurtosis and the coefficient of variation.

The corresponding computation indicates that the greatest eigenvalue of the judgment matrix is 8.0212, and the corresponding greatest eigenvector of the judgment matrix is W'=(0.4808, 0.4808, 0.4808, 0.3302, 0.1717, 0.1717, 0.1717, 0.3302).

The values of the consistency indicator and consistency

ratio can be computed as follows: CI = 0.003 and CR = 0.0021 ≤ 0.1. The consistency ratio clearly meets the requirement. Therefore, the results of the hierarchical single arrangement are consistent and meet the consistency check requirement.

After the normalisation of the greatest eigenvector, the weights of the multi-features are W = (0.1837, 0.1837, 0.1837, 0.1261, 0. 0656, 0. 0656, 0.0656, 0.1261).

4.3 The analysis results of warning

Based on the above values and weights of the multi-features, the Euclidean distance can be obtained from a comparative analysis of the monitored waveforms and the reference waveforms. The Euclidean distances of different sliding windows are shown in Fig. 7.

Based on the Euclidean distances in Fig. 7, the similarity between the monitored waveforms and reference waveforms can be computed with Formula (8).

The static thresholds of similarity can be set manually according to the actual needs of the operation. In this case, the static thresholds of grade 2 and grade 1 are set to 95% and 85%, respectively. Based on these static thresholds and the fluctuation degree of the similarity waveform, the dynamic thresholds can be computed using Formula (9).

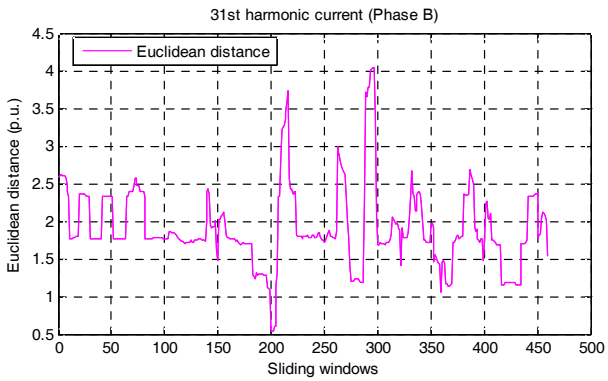

Fig. 7. Euclidean distances between the monitored waveforms and the reference waveforms

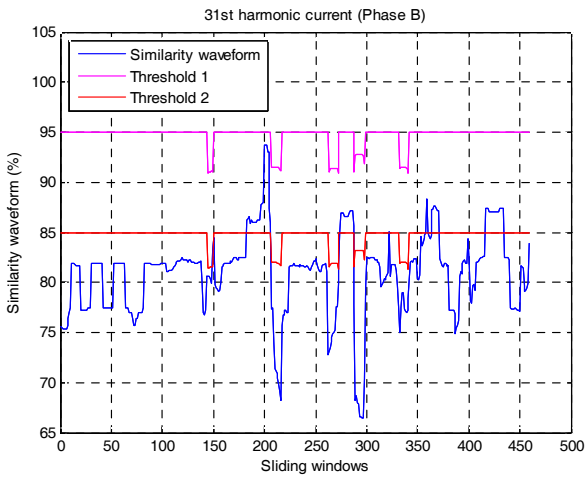

Fig. 8. Similarity waveform and dynamic thresholds waveform

The results of the similarity waveform and the dynamic thresholds are shown in Fig. 8.

The above waveform intuitively shows the limit-exceeding information of the similarity. After a contrastive analysis, the specific number and ratio of limit-exceeding instances can be computed. The results are shown in Table 2.

Table 2. The Results of Contrastive Analysis

Category / Results	Number of over 95%	Ratio of over 95%	Number of over 85%	Ratio of over 85%
Similarity	0	0	67	14.5970%
Normality	328	70%	422	90%

According to the information in Table 2, the number of limit-exceeding instances cannot meet the requirement of normality when the aspect of ratio exceeds 95% or 85%. Therefore, the abnormal degree of the case can be given a PQ warning of grade 2.

In addition to the 31st harmonic current, other PQ indictors can be executed for abnormal data mining and given the corresponding warning prompts by using the above analysis method. The PQ warning analysis results of all abnormal indictors at the above monitored point in the same day are shown in Table 3.

Table 3. The Analysis Results of Other PQ Indictors

Category / Indictors	Phase	Ratio of over 95%	Ratio of over 85%	Grade of warning
31st harmonic current	A	0	3.9216%	2
31st harmonic current	B	0	14.5970%	2
31st harmonic current	C	1.7429%	47.4945%	2
negative sequence current	/	68.3716%	91.0256%	1
voltage fluctuation	A	87.6068%	95.0855%	Normality
voltage fluctuation	B	65.3846%	92.9487%	1
voltage fluctuation	C	77.9915%	90.3846%	Normality

4.4 Comparison with the existing warning approach

At present, there are not many papers or approaches that can analyse the abnormal severity of PQ problems and give warning prompts. This paper uses the method in [28] to compare with the proposed approach. Based on the same example, the analysis results computed by the method in [28] are shown in Table 4.

Through the analysis results comparison between Table 3 and Table 4, it can be found that even though grades of warning are not completely same, two methods all judge the same PQ data as abnormal data. Meanwhile, phase A and phase C of voltage fluctuation are all judged as normal data by two methods. Based on these analyses, it shows that the things two methods have in common are both of two methods can distinguish the same PQ abnormal and normal data, and give reasonable warning prompts.

Table 4. The Analysis Results of the Method in [28]

Indictors \ Category	Phase	Limit-exceeding proportion	95% probability value	Maximum of product	Grade of warning
31st harmonic current	A	19.4444%	/	/	4
31st harmonic current	B	17.5214%	/	/	4
31st harmonic current	C	35.0427%	/	/	4
negative sequence current	/	2.1368%	1.1258A	4579.6259	2
voltage fluctuation	A	0.0064%	0.8589%	50.1257	Normality
voltage fluctuation	B	1.7094%	2.2573%	3124.8634	2
voltage fluctuation	C	1.0684%	1.5026%	75.2635	Normality

Compared with the method in [28], the proposed approach in this study has the following differences: 1) Two methods adopt different PQ warning mechanisms. The most serious warning grades in two methods are grade 4 and grade 2 respectively. This is the main reason why two methods can distinguish the same PQ abnormal data and give different grade of warning. 2) Two studies use different PQ warning methods to perform anomaly detection. Based on the change characteristics of multi-features, this paper utilizes similarity to analyse the abnormal severity. It can better reflect anomalous change of monitored data of one specific PQ disturbance source. 3) This study sets dynamic thresholds to perform a PQ warning. It can overcome the normal jitter of monitored data and increase accuracy of PQ warning.

5. Conclusions

Based on the PQ characteristic analysis for HSR, the typical PQ problems for HSR become explicit in this study. A warning approach based on multi-features similarity and the hierarchical PQ warning flow is applied to mine abnormal problems of PQ monitored data. Taking the PQ warning for one 220 kV I-bus bar at one traction substation access point as an example, the accuracy and effectiveness of the proposed algorithm and flow process has been verified.

The approach proposed in this study and the analysis results can also be used to conduct HSR PQ warnings, serve as the supplement and perfect the existing PQ monitoring system. As such, all types of PQ abnormal changes in the HSR can be identified and warnings issued in a timely manner. Finally, the power grid and the railway authorities can avoid the evolution of an accident and effectively improve its reliability and economy by taking necessary counter measures.

Acknowledgements

This work was supported in part by the National High Technology Research and Development Program of China (863 Program Grant No. 2011AA05A107), the National Science Foundation of China (Grant No. 51277027), and the State Grid Corporation of China (2013-Power Quality Warning).

References

[1] A. Bueno, J. M. Aller , J. A. Restrepo, et al, "Harmonic and unbalance compensation based on direct power control for electric railway systems," *IEEE Trans on Power Electron*, Vol.28, No.12, pp. 5823-5831, Dec. 2013.

[2] C. Wu, A. Luo, J. Shen, F. J. Ma, et al, "A negative sequence compensation method based on a two-phase three-wire converter for a HSR way traction power supply system," *IEEE Trans on Power Electron*, Vol. 27, No. 2, pp. 706-717, Feb. 2012.

[3] G. W. Chang, H. W. Lin, S. K. Chen, "Modeling characteristics of harmonic currents generated by HSR way traction drive converters," *IEEE Trans on Power Del*, Vol. 19, No. 2, pp. 766-733, Apr. 2004.

[4] M. Brenna, F. Foiadelli, D. Zaninelli, "Electromagnetic model of high speed railway lines for power quality studies," *IEEE Trans on Power Syst*, Vol. 25, No. 3, pp. 1301-1308, Aug. 2010.

[5] C.C. Shen, C.N. Lu, "A voltage sag index considering compatibility between equipment and supply," *IEEE Trans on Power Del*, Vol. 22, No. 2, pp. 996-1002, Apr. 2007.

[6] A. McEachern, "Designing electronic devices to survive power-quality events," *IEEE Industry Applications Magazine*, Vol. 6, No. 6, pp. 66-69, Nov-Dec. 2000.

[7] M. Brenna, F. Foiadelli, D. Zaninelli, "Electromagnetic model of high speed railway lines for power quality studies," *IEEE Trans on Power Syst*, Vol. 25, No. 3, pp. 1301-1308, Aug. 2010.

[8] A. Capasso, G. Ghilardi, G. G. Buffarini, "Bologna-Florence high speed railway line: MV emergency traction power supply, operating conditions and PQ issues," *in Proceeding of IEEE_ESARS,* pp.1-5, 2010.

[9] F. Ciccarelli, M. Fantauzzi, D. Lauria, "Special transformers arrangement for AC railway systems," *in Proceeding of IEEE_ESARS*, pp.1-6, 2012.

[10] M. Gupta, R. Kumar, R. A. Gupta, "Neural network based indexing and recognition of power quality disturbances," *Telkomnika*, Vol. 9, No. 2, pp. 227-236, Aug. 2011.

[11] S. He, K. Li, M. Zhang, "A real-time power quality disturbances classification using hybrid method based on s-transform and dynamics," *IEEE Trans on In-*

strumentation and Measurement, Vol. 62, No. 9, pp. 2465-2475. 2013.
[12] G. Li, G. Li, X. Fu, et al, "Synthetic evaluation of power quality based on entropy of relative intensity and local variable weight," *Power System Technology (POWERCON), 2010 International Conference*, pp. 1-6, Oct. 2010.
[13] Y. Hai, J. Chen, "Power quality evaluation based on wavelet packet decomposition and fuzzy logic," *Computer Science and Automation Engineering (CSAE), 2012 IEEE International Conference*, pp. 504-507, May. 2010.
[14] M. Simic, D. Denic, D. Zivanovic, et al, "Development of a data acquisition system for the testing and verification of electrical power quality meters," *Journal of Power Electronics*, Vol. 12, No. 5, pp. 813-820, Sep. 2012.
[15] K. Yingkayun, S. Premrudeepreechacharn, "A power quality monitoring system for real-time detection of power fluctuations," *in Proc. IEEE 40th North Am erican Power Symposium*, pp. 53-57, 2008.
[16] Z. W. Zhang, B. Wu, J. S. Kang, et al, "A multi-purpose balanced transformer for railway traction applications," *IEEE Trans on Power Del*, Vol. 24, No. 2, pp. 711-718, Apr. 2009.
[17] S. L. Chen, R. J. Li, P. H. Hsi, "Traction system unbalance problem analysis methodologies," *IEEE Trans on Power Del*, Vol. 19, No. 4, pp. 1877-1883, Oct 2004.
[18] S. A. Yin, C. L. Su, R. F. Chang, "Assessment of power quality cost for high-tech industry," *in Proc. I EEE Power India Conference*, pp. 927-932, 2006.
[19] Z. L. Shu, S. F. Xie, Q. Z. Li, "Single-phase back-to-back converter for active power balancing, reactive power compensation, and harmonic filtering in traction power system," *IEEE Trans on Power Elec*, Vol. 26, No. 2, pp. 334-343, Feb. 2011.
[20] P. Moallem, A. Zargari, A. Kiyoumarsi, "Improvement in computation of delta V-10 flicker severity index using intelligent methods," *Journal of Power Electronics*, Vol. 11, No. 2, pp. 228-236, May. 2011.
[21] A. Zheng, J. Li, J. Liu, et al, "One definition method for abnormal thresholds in steady-state power quality early warning," C.N. Patent, 201110067687.7, Mar. 21, 2011.
[22] J.B. McDonald, J. Sorensen, P.A. Turley, "Skewness and kurtosis properties of income distribution models," *Review of Income and Wealth*, Vol. 59, No. 2, pp. 360-374, Jun. 2013.
[23] J. H. Estrada, E. A. Cano-Plata, C. Younes-Velosa, et al, "Entropy and coefficient of variation (CV) as tools for assessing power quality," *Ingenieria e Investigacion*, Vol. 31, No. 2, pp. 31: 45-50, Oct. 2011.
[24] X. Yuan, J. Zhao, G. Tang, et al, "Multi-level fuzzy comprehensive evaluation of power quality," *in Proceeding of IEEE_DRPT*, Vol. 1, pp. 290-294, 2004.
[25] AI. Chatzimouratidis, PA. Pilavachi, "Multicriteria evaluation of power plants impact on the living standard using the analytic hierarchy process," *Energy Policy*, Vol. 36, No. 3, pp. 1074-1089, Apr. 2008.
[26] S. Mishra, C. N. Bhende, B. K. Panigrahi, "Detection and classification of power quality disturbances using S-transform and probabilistic neural network," *IEEE Trans on Power Del*, Vol. 23, No. 1, pp. 280-287, Jan. 2008.
[27] B. K. Panigrahi, V. Ravikumar Pandi, "Optimal feature selection for classification of power quality disturbances using wavelet packet-based fuzzy k-nearest neighbour algorithm," *Generation, Transmission & Distribution, IET*, Vol. 3, No. 3, pp. 296-306, Mar. 2009.
[28] W. Gu, J. Bai, X. Yuan, et al, "Power Quality Early Warning Based on Anomaly Detection," *Journal of Electrical Engineering & Technology*, Vol. 9, No. 4, pp. 1171-1181, Jul. 2014.

Jingjing Bai received the B.Eng. degree in Electrical Engineering from Jiangsu University, China in 2012. He is currently pursuing the M.Eng degree in Electrical Engineering at Southeast University. His research interest is power quality.

Wei Gu received his B.Eng degree and Ph.D. degree in Electrical Engineering from Southeast University, China, in 2001 and 2006. From 2009 to 2010, he was a Visiting Scholar in the Department of Electrical Engineering, Arizona State University, Tempe, AZ 85287, USA. He is now a professor in the School of Electrical Engineering, Southeast University. His research interests are power system stability and control, smart grid, renewable energy technology and power quality.

Xiaodong Yuan received the B.S. and M.S. degrees from Southeast University, China, in 2002 and 2005, respectively. Currently he is a director with new energy and distribution network laboratory, Jiangsu Electrical Power Company Research Institute, China. He is now taking the responsibility of smart distribution power system, renewable energy technology and power quality.

Qun Li received the Ph.D. degree from Southeast University, China, in 1998. Currently he is a director with power grid technology center, Jiangsu Electrical Power Company Research Institute, China. He is now taking the responsebility of smart distribution power system, renewable energy technology and power quality.

Bing Chen received the Ph.D. degree from China. Currently he is a senior engineer with new energy and distribution network laboratory, Jiangsu Electrical Power Company Research Institute, China. He is now taking the responsibility of smart distribution power system, renewable energy technology and power quality.

Xuchong Wang received the B.Eng degree in Electrical Engineering from Southeast University, China in 2013. He is currently pursuing the M.Eng degree in Electrical Engineering at Southeast University. His research interest is power quality.